White Rose Research Online

eprints@whiterose.ac.uk
https://eprints.whiterose.ac.uk
Universities of Leeds, Sheffield and York

Deposited via The University of Sheffield.

White Rose Research Online URL for this paper:
https://eprints.whiterose.ac.uk/id/eprint/164205/

Version: Accepted Version

Article:
Ghazizadeh, S., Hanein, T., Provis, J.L. et al. (2020) Estimation of standard molar entropy of cement hydrates and clinker minerals. Cement and Concrete Research, 136. 106188. ISSN: 0008-8846

https://doi.org/10.1016/j.cemconres.2020.106188

Article available under the terms of the CC-BY-NC-ND licence (https://creativecommons.org/licenses/by-nc-nd/4.0/).

Reuse
This article is distributed under the terms of the Creative Commons Attribution-NonCommercial-NoDerivs (CC BY-NC-ND) licence. This licence only allows you to download this work and share it with others as long as you credit the authors, but you can't change the article in any way or use it commercially. More information and the full terms of the licence here: https://creativecommons.org/licenses/

Takedown
If you consider content in White Rose Research Online to be in breach of UK law, please notify us by emailing eprints@whiterose.ac.uk including the URL of the record and the reason for the withdrawal request.

UNIVERSITY OF LEEDS
University of Sheffield
UNIVERSITY of York

Estimation of standard molar entropy of cement hydrates and clinker minerals

Sam Ghazizadeh[a]*, Theodore Hanein[a], John L. Provis[a], Thomas Matschei[b]*

[a] Department of Materials Science and Engineering, The University of Sheffield, Sir Robert Hadfield Building, Sheffield S1 3JD, United Kingdom
[b] RWTH Aachen University, Department of Civil Engineering, Institute of Building Materials Research, 52062 Aachen, Germany

ABSTRACT

It is not straightforward to experimentally measure the standard molar entropy of cement hydrates or clinker minerals. This is further compounded by the controversies surrounding the entropy values reported in established thermodynamic datasets for cements. The purpose of this study is to assess the reliability of standard entropies compiled in those datasets. To this end, a simple but robust method is used in which the standard entropy of an inorganic solid is correlated to its formula unit volume via a linear equation. The results of this analysis show that the standard entropies and/or molar volumes (and in cases solubility products) of the following phases deserve closer scrutiny: meta-ettringite phases; magnesium/aluminium layered double hydroxide solid solutions; almost all iron-bearing monosulfate and hydrogarnet phases; and several calcium silicate hydrate solid solution end-members. In addition, this study reports the provisional estimates for the standard entropies of minerals ternesite and ye'elimite.

Keywords: Thermodynamic, Standard entropy, Cement

1. Introduction

Thermodynamics has long been crucial to materials science, with the field of cement being no exception. The past two decades have seen more uses of thermodynamics in studying cements, but the key advancements include the equilibrium calculations of cement clinkering [1,2] and of the hydration of cements which occur at much lower temperatures [3,4]. Progress has been made at pace with respect to the latter where the interest lies in predicting the phase assemblage of hydrating cements at standard pressure but over a wide range of temperatures from 10 to 100 °C. In most studies, cements are not the only reacting solids in the system, but they coexist with inorganic salts, natural minerals and/or industrial by-products of various chemical compositions. Overall, it is fairly complex to model these materials in reactions with water. This is in part due to the lack of thermodynamic data

Cement oxide notations used in this paper are: A=Al_2O_3; C=CaO; F=Fe_2O_3; H=H_2O; M=MgO; S=SiO_2; c=CO_2; s=SO_3

* Corresponding authors
Email addresses: sam.ghazizadeh@sheffield.ac.uk (S. Ghazizadeh), t.hanein@sheffield.ac.uk (T. Hanein), j.provis@sheffield.ac.uk (J. Provis), matschei@ibac.rwth-aachen.de (T. Matschei)

for some of the compounds that are expected to form during the hydration of a given cement system, in particular when constituents other than Portland cement are present, or at temperatures other than 25 °C. The accuracy of some of the existing data is also open to question, which further complicates the problem.

To perform the equilibrium calculations of hydration, the common practice is to use available software packages (such as GEMS [5,6] or PHREEQC [7]) coupled with thermodynamic databases developed specifically for cements. Thermodynamic properties of several cement hydrates and clinker minerals, especially as relates to Portland cement (and its blends) and alkali-activated materials, are compiled into two major datasets; *Cemdata* [3,8,9] and *Thermoddem* [10,11]. These databases report the value of Gibbs free energy of formation, enthalpy of formation, entropy, heat capacity, molar volume and equilibrium solubility products for substances and reactions pertaining to cements. All reported data are for the standard temperature and pressure of 298.15 K and 1 bar albeit the heat capacities are given as a function of temperature, valid up to 100 °C. The accuracy of reported data is essential to performing reliable thermodynamic calculations.

The complete thermodynamic properties of a material can be constructed by combining experimentally obtained entropy, enthalpy and heat capacity data. Amongst these parameters, entropy at a reference temperature (for example at 298.15 K for standard entropy) is difficult to measure. To experimentally derive the standard entropy of a material, the third law of thermodynamics needs to be followed; that is, to measure the isobaric heat capacity (C_p) over a range of temperatures (T) from near 0 K to above 298.15 K, and then integrate the C_p/T function with respect to T from 0 K to 298.15 K. This method is hardly ever used in the cement literature to derive the standard entropy of cement hydrates, possibly because (i) the experimental setup required for the direct determination of heat capacity to near absolute 0 is not widely available, and (ii) it is difficult to prepare cement hydrates (and their selected end-members) in a sufficiently pure form so that to enable precise measurements. The alternative approach commonly used is to measure the equilibrium solubility product of hydrates at multiple temperatures, then to fit the standard entropy term within the so-called three-term approximation equation to the measured solubility data (for more detail, see [12] or Section 3 of this paper). The entropy value that gives the best fit to the measured solubility data is deemed to be the one representing the hydrate in question.

The three-term approximation method may lead to inaccurate entropy values if it happens that the measured solubility products are missing, incorrect (or subject to significant uncertainty), or somehow fail to represent the hydrates studied. No matter how meticulously experiments are performed, there exists a possibility that the measured solubility product represents a condition in which the solution is not in equilibrium with respect to the hydrate, but rather

is influenced by one or more remnant precursor materials and/or metastable phases. Unfortunately, the accuracy of entropy data obtained to date via this method is rarely assessed using independent techniques (although a few exceptions exist, *e.g.* [13]). Therefore, an issue arises regarding whether the standard entropies and equilibrium solubility data of substances reported in established thermodynamic databases for cements are accurate and reliable – and this poses a significant challenge.

Given the paucity of experimental entropy data, and the labour-intensive and complex processes involved in obtaining and assessing them, it would be very valuable to estimate the standard entropy using methods that have solid thermodynamic grounds but are independent of the experimental procedures used so far.

The purpose of this study is to examine the accuracy of standard entropies of cement hydrates and clinker minerals given in *Cemdata18* [3]. This dataset is chosen as it contains more hydrates than *Thermoddem* [10,11]; however, discrepancies between the two are also discussed.

In what follows, we first present a description of various methods to estimate standard entropy. Then, a simple method is employed and compared against the published entropy data. The method is also used to derive the standard entropy of ye'elimite and ternesite. These are clinker minerals that have been under rigorous investigation recently due to their potential environmental and economic benefits [14]; however, their standard entropy is still unknown.

2. Estimation of standard entropy

Methods to find estimates of standard entropy are numerous, with some dating back to as early as the 1920s. Their use is also relatively familiar in the field of cement science. For instance, in 1985, Babushkin *et al.* [15], who for the first time compiled a relatively comprehensive thermodynamic dataset for cement substances, adopted a few of those methods. It is not our intention to comprehensively review all such methods in detail, but the key methods that have already been applied to cements or have the potential to be used in the future, are discussed here.

By far the most widely used type of method to estimate the standard entropy of inorganic minerals and hydrates consists of a mathematical relationship in which the standard molar entropy of a compound is related to [15–19]:

(i) the sum of the standard molar entropies of the constituent oxides and hydroxides, or
(ii) a weighted sum of the standard molar entropies and standard molar volumes of the constituent oxides and hydroxides, or
(iii) only the standard molar volume of the solid in question.

The first two of these are known as *additivity methods* and take the forms given by Eq. 1 or Eq. 2, respectively:

$$S^{\circ}_{298,\mathrm{j}} = \sum_{\mathrm{i}=1}^{\mathrm{x}} \mathrm{n_i} S^{\circ}_{298,\mathrm{i}}, \quad (1)$$

$$S^{\circ}_{298,\mathrm{j}} - \mathrm{k'} V_{\mathrm{molar,j}} = \sum_{\mathrm{i}=1}^{\mathrm{x}} \mathrm{n_i} (S^{\circ}_{298,\mathrm{i}} - \mathrm{k'} V_{\mathrm{molar,i}}), \quad (2)$$

where $S^{\circ}_{298,j}$ and $V_{molar,j}$ are the standard molar entropy and molar volume of the inorganic compound of interest, n_i is the stochiometric coefficient of the ith constituent species within this compound, $S^{\circ}_{298,i}$ and $V_{molar,i}$ are the standard molar entropy and molar volume, respectively, of the constituent oxide or hydroxide. k' is a constant and its value depends on the constituent type and their coordination state. Holland [16] has further simplified Eq. 2, by showing that k' can be approximated to 1 as $\partial S/\partial V$ at 298.15 is close to unity. Eq. 1 has been more common than Eq. 2 in the cement literature, and has previously been used, for instance, by Myers *et al.*, to estimate the standard entropy of several end-members of the calcium (sodium) aluminosilicate hydrate solid solution which can occur in Portland cement blends and alkali activated cements [20,21].

It is worth noting that the standard molar entropy of a compound is related to its heat capacity; factors that affect the latter will also affect the former (and are known to be significant at temperatures near 298.15 K [17]). Considering this, Eq. 2 can yield relatively smaller errors than Eq. 1, as it enables one to account for factors that influence standard entropy. This includes the effect of volume, coordination state and/or magnetic order-disorder transformation which specifically occurs in minerals with transition metals [16,17]. To correct for these, different $S^{\circ}_{298} - k' V_{molar}$ can be adopted for different coordination states, thereby also allowing for the correction of the magnetic disorder. The absence of this from Eq. 1, and its consequent influence on estimating the entropy, becomes particularly evident when different polymorphs of the same composition are to be analysed. Using Eq. 1 leads to identical standard entropies for different polymorphs, because their selected oxide or hydroxide constituents are the same. However, it is not really possible for two (or more) polymorphs with the same chemical composition (*i.e.* undoped) to have the same standard entropy. This is due to the fact that different structures have different heat capacity and thus entropy. In spite of their popularity, Eq. 1 and Eq. 2 are not straightforward to use as they require very careful consideration in the selection of the constituent oxides or hydroxides.

Using a somewhat similar principle to that embodied by Eq. 1, it has become customary in the cement literature to estimate the standard entropy of a solid by assuming a reference (usually fictive) reaction involving compounds of known entropies and with a net zero entropy ($\Delta_r S^{\circ}$=0), where reactants and

products are structurally analogous to each other [10,22]. This method was first proposed by Helgeson in 1978 [23]. For instance, in order to approximate the standard entropy of Fe-bearing ettringite, one can write Fe-ettringite + $Al_2O_3 \rightarrow$ Al-ettringite + Fe_2O_3. The shortcoming of this method (in addition to those pertinent to Eq. 1) is that errors can arise and propagate if the entropies of the reference compounds are already inaccurate, or if the compounds are not selected carefully. This is specifically important in the case of hydrates, as the binding state of water (*e.g.* whether it is easily removable zeolitic water or structurally bound) has a significant influence on the entropy estimations.

The third type of estimation method concerns a simple relationship whereby the standard entropy of an inorganic solid is directly correlated to its molar volume. A seemingly rather simple form of such relationships was developed by Turkdogan and Pearson [24] in 1953, which was later recommended by Babushkin *et al.* in their book [15]:

$$S^{\circ}_{298} = a.V^{n}_{molar} \quad (3)$$

where V_{molar} is molar volume, a and n are variables and their values depend on several factors such as the crystal structure, cation-anion ratio, the cation group in the periodic table, and the nature of the anions (whether oxides, silicates, sulfates or carbonates). However, Turkdogan and Pearson [24] could not systematically establish how the constants would be defined from fundamental principles, mainly because they had access to an insufficient body of thermodynamic data at the time. Their method was therefore proven difficult to apply in estimating the entropy of material classes for which a and n did not exist (or were not able to be fitted to existing databases).

Recently, Jenkins and Glasser established a new volume-based relationship [25–27] which is much simpler than Eqs. 1-3. In their studies, the authors found that the standard entropies of inorganic minerals and hydrates obey a distinct relationship in which entropy is an increasing function of formula unit volume. The general form of their relationship is presented in Eq. 4:

$$S^{\circ}_{298} = kV_m + c \quad (4)$$

where V_m is the formula unit volume (nm^3·formula-$unit^{-1}$), and *k* and *c* are empirically determined constants. There are several ways to calculate V_m [28], but the easiest is to use Eq. 5:

$$V_m = V_{molar} \times 10^{21}/N_A \quad (5)$$

where V_{molar} (cm^3·mol^{-1}) can be readily retrieved from most thermodynamic databases (including those related to cementitious systems), and N_A is the Avogadro constant (6.022 × 10^{23} formula-unit·mol^{-1}). Jenkins and Glasser derived Eq. 4 (which has thermodynamic basis; $\partial S/\partial V$ is constant at a given pressure [25]) by the regression analysis of a standard dataset involving inorganic materials with different stoichiometries. Fig. 1 shows the data used in their analysis. The filled circles represent 67 inorganic ionic hydrates (*e.g.*

$CaSO_4 \cdot 2H_2O$) whereas the hollow circles are 94 anhydrous minerals. From these data, the authors of those studies identified that the values of the fitted constants in Eq. 4 depend on whether the inorganic solids are hydrated or anhydrous. Their two resulting equations are Eq. 6 and Eq. 7, providing a simple means to estimate standard molar entropy (note that there are errors associated with such estimates; 7.4% for Eq. 6 and 12.6% for Eq. 7 [25]).

$$S^{\circ}_{298} = 1579\ V_m + 6; \text{ for solid hydrates} \quad (6)$$

$$S^{\circ}_{298} = 1262\ V_m + 13; \text{ for anhydrous inorganic minerals} \quad (7)$$

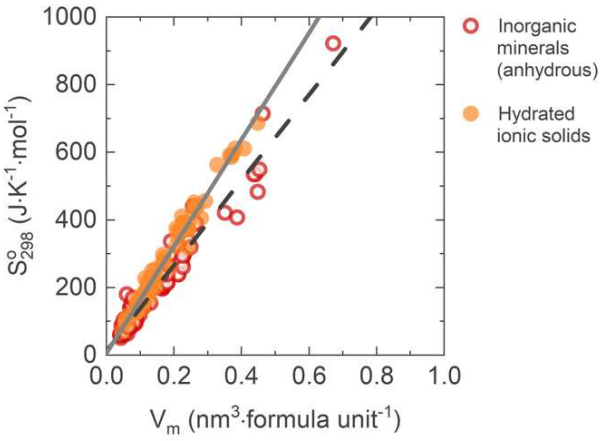

Fig. 1: Standard molar entropy versus formula unit volume, for inorganic minerals (anhydrous) and hydrated ionic solids, reproduced from the dataset given in [25]. The dashed and solid lines are the result of regression analysis carried out by Jenkins and Glasser on each given dataset.

Following on from their earlier work, Jenkins and Glasser [26,27,29,30] have also established that the standard molar entropy of a hydrated mineral (*e.g.* $CaSO_4 \cdot 2H_2O$) is linearly correlated to that of its anhydrous counterpart (*e.g.* $CaSO_4$), via Eq. 8:

$$S^{\circ}_{298}\{X \cdot mH_2O\} - S^{\circ}_{298}\{X\} = m\theta_{S^{\circ}_{298}} \quad (8)$$

where X denotes the anhydrous crystal, m is the number of water molecules in the hydrated crystal, and $\theta_{S^{\circ}_{298}}$ is a constant. Eq. 8 is identical to the concept underpinning the additivity methods in Eq. 1 and Eq. 2, where entropy is seen as an additive quantity of the constituents. Water is one of the constituents of hydrates and so could be defined separately as a component of Eq. 1 or Eq. 2. Jenkins and Glasser investigated 83 salt pairs in [31] and determined a value of $\theta_{S^{\circ}_{298}}$ = 40.9 J·K^{-1}·mol^{-1}·(H_2O molecule)$^{-1}$, regardless of the composition of the parent salt. As an example, Fig. 2 shows the standard entropy of $CaSO_4 \cdot mH_2O$ as a function of the number (m) of water molecules in its formula. The hollow circles are the standard entropies measured experimentally, whereas the solid line represents Eq. 8. The entropy data are an increasing function of water content, and Eq. 8 fits these data very well. The same has been observed for other 83 salt pairs, with correlation

coefficient r^2 being equal to 0.978 [31]. Nevertheless, the possible downside of Eq. 8 with a fixed constant of $\theta_{S^\circ_{298}}$ = 40.9 J·K^{-1}·mol^{-1}·(H$_2$O molecule)$^{-1}$ is that it only represents one state of water in the crystal structure; this will be discussed further in Section 3.4.

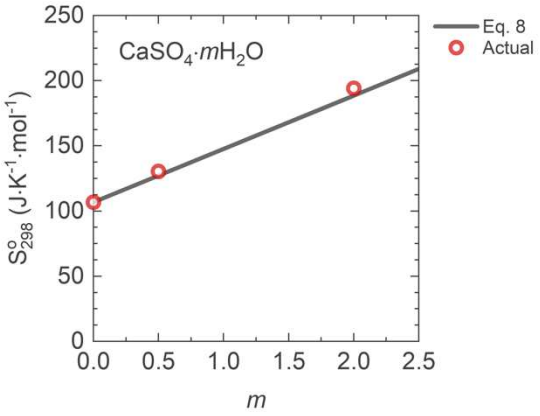

Fig. 2: Standard molar entropy of $CaSO_4 \cdot mH_2O$ as a function of the number of formula water. Data points are retrieved from [31]. Solid line is the estimation of standard entropy based on Eq. 8 where $\theta_{S^\circ_{298}}$ = 40.9 J·K^{-1}·mol^{-1}·(H$_2$O molecule)$^{-1}$.

Compared to Eq. 1 and Eq. 2, Jenkins and Glasser's method is easy to apply and has already been used for a variety of problems [30]. The only parameter required in their approach is the formula unit volume, leading to calculations which are simple to execute. However, this simplicity comes at a price. Eq. 4 compromises the accuracy of predicted standard entropy, compared to Eq. 2 where additional $S^\circ_{298} - k'V_{molar}$ terms could be incorporated (if necessary) to correct for the factors that affect standard entropy [16,17]. An example where Eq. 4 falls short is with respect to the standard entropies of minerals larnite and calcium olivine (which are the β and γ polymorphs of Ca_2SiO_4, respectively). The standard molar entropies of these materials, as measured experimentally, are 127.61 J·mol^{-1}·K^{-1} and 120.5 J·mol^{-1}·K^{-1}, respectively; however, their formula unit volumes are 0.085 nm^3·formula-unit^{-1} and 0.098 nm^3·formula-unit^{-1} (see data in supporting information of [25]). Eq. 4 would predict a lower entropy for larnite based on its lower formula unit volume, but the reverse is true. The aluminosilicate minerals andalusite and sillimanite (both polymorphs of Al_2SiO_5) also show this type of inverted relationship (see supporting data given in [25]). Nonetheless, such cases are rare; generally, the differences in standard entropies caused by factors other than change of molar volume are small [16,17].

Equations 6-8 can be useful in the thermodynamics of cement hydrates and clinker minerals. The application of these equations is twofold: (i) to assess the reliability of standard entropies already acquired via experiments, or (ii) to estimate standard entropies (even if provisionally) when it is difficult to measure them directly. Either way, errors associated with the use of Eq. 6-8

are small, based on the statistical estimates of uncertainties given in [25] for a wide range of mineral phases.

Equation 8 can also play an important role in estimating standard entropies of hydrates with different water contents, especially when the entropy value of a specific hydration level is required (and when molar volume is not known to high precision, preventing the use of Eq. 6). It has occurred in the past that studies derived the standard entropy of a hydrate with specific water content, but then struggled to compare their findings with other datasets (see *e.g.* [13]).

In the following sections, we take the standard entropies of cement hydrates and clinker minerals in [3], and plot them against their corresponding formula unit volumes. Therein, Eq. 6 or Eq. 7 is also plotted for comparison. Where the relationship between the standard entropy and formula unit volume falls significantly away from the lines defined by Eq. 6 or Eq. 7, it is possible that errors are associated with one or both of these parameters, and the possible reasons for such errors are therefore explored. Discussions are also included when discrepancies are found between *Cemdata18* [3] and *Thermoddem* [10,11] datasets.

3. Cement hydrates

3.1 AFt phases

The standard molar entropies and formula unit volumes of all AFt hydrates listed in [3] are shown in Fig. 3. The solid line represents Eq. 6, which is applicable to hydrous phases. The main observation from Fig. 3 is that there are only two data points which are not described accurately by Eq. 6: the ettringite hydrates with $13H_2O$ and $9H_2O$ water contents. The reason for this is as follows.

3.1.1 meta-ettringite

The standard entropies of these phases were originally derived by Baquerizo *et al.* [32], by examining how ettringite ($C_6As_3H_{32}$) decomposes or reforms as relative humidity and temperature change. Those authors made an interesting observation, consistent with an earlier study by Zhou and Glasser [33], that $C_6As_3H_{32}$ loses water as relative humidity reduces, thereby transforming to $C_6As_3H_{13}$ or $C_6As_3H_9$ (these phases are generally referred to as meta-ettringite). However, once they are exposed to increased levels of relative humidity, ettringite reforms, but following a pattern which is distinct from that of decomposition. This pattern is shown in Fig. 4.

Unfortunately, this behaviour of ettringite made it difficult for Baquerizo *et al.* [32] to derive the exact standard entropies of $C_6As_3H_{13}$ or $C_6As_3H_9$. To better appreciate why, their method is briefly discussed here.

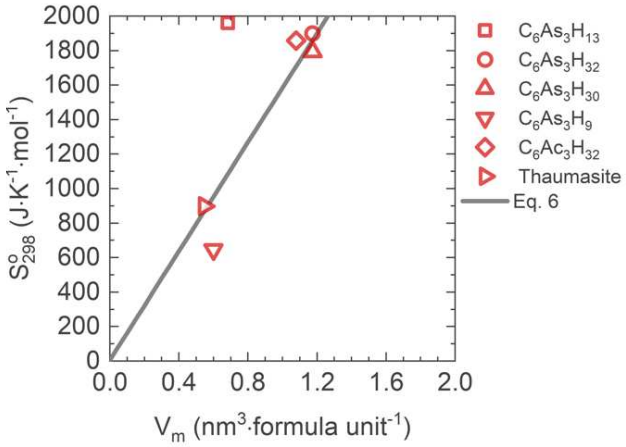

Fig. 3: Standard molar entropy (from [3]) plotted against formula unit volume, for AFt hydrates. Formula unit volumes were calculated using Eq. 5 and the molar volumes tabulated for these phases in Table 1 of [3]. The solid line is Eq. 6.

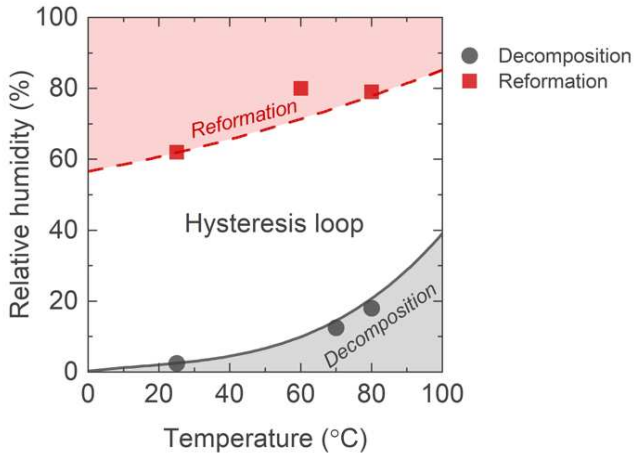

Fig. 4: Stability of ettringite as a function of relative humidity and temperature, for reactions given in Eq. 9 and Eq. 10 as defined in the text; data are from [32]. The dots represent the data obtained experimentally, whereas the solid and dashed curves result from the thermodynamic model developed in [32]. The true thermodynamic equilibrium for $C_6As_3H_{13}$ is believed to be somewhere within the hysteresis loop (not shown here, but an estimate of the zero-hysteresis line was made by Baquerizo *et al.* in their article [32]).

To calculate the standard entropy of $C_6As_3H_{13}$, the authors of [32] followed reactions given in Eq. 9 and Eq. 10:

$$C_6As_3H_{13} + 17H_2O \rightarrow C_6As_3H_{30} \quad (9)$$

$$C_6As_3H_{30} \rightarrow C_6As_3H_{13} + 17H_2O \quad (10)$$

and determined the equilibrium relative humidity at different temperatures for these reactions. Thereafter, the equilibrium points, shown in Fig. 4, were entered into the van't Hoff equation (Eq. 11) to calculate $\Delta_r H°$:

$$\frac{\partial(\ln K_{eq})}{\partial(1/T)} = \frac{-\Delta_r H°}{R} \quad (11)$$

where K_{eq} is the equilibrium constant, R is the gas constant (8.31451 J·mol^{-1}·K^{-1}) and T is the temperature in Kelvin. The Gibbs free energy ($\Delta_r G°$) of the reactions was then calculated using Eq. 12:

$$\Delta_r G° = -RT \ln K_{eq} \quad (12)$$

and $\Delta_r S°$ was subsequently obtained via Eq.13:

$$\Delta_r G° = \Delta_r H° - T\Delta_r S° \quad (13)$$

The standard entropy of $C_6As_3H_{13}$ could then be simply calculated using the standard entropies of water and $C_6As_3H_{30}$. A similar procedure was also used to calculate the standard entropy of $C_6As_3H_9$ but considering the reaction in Eq. 14:

$$C_6As_3H_{13} \rightarrow C_6As_3H_9 + 4H_2O \quad (14)$$

Taking $C_6As_3H_{13}$ as an example, since the formation and decomposition of this phase follow two different patterns (as seen in Fig. 4), the calculations via Eqs. 11-13 would lead to two different quantities of standard entropy for $C_6As_3H_{13}$; that is 710.6 J·K^{-1}·mol^{-1} for Eq. 9 and 1960 J·K^{-1}·mol^{-1} for Eq. 10. The key question is which entropy value should be taken as the standard entropy of $C_6As_3H_{13}$ – in principle the answer is that neither of these should be, as neither Eq. 9 nor Eq. 10 represents the true equilibrium conditions with respect to $C_6As_3H_{13}$ formation. The same argument applies to $C_6As_3H_9$.

In light of Fig. 3 and the procedure outlined above, it becomes clear that the entropies of $C_6As_3H_{13}$ and $C_6As_3H_9$ derived by Baquerizo *et al.* [32] should have been expected to depart far from their equilibrium values.

According to Eq. 6, the standard entropies of $C_6As_3H_{13}$ and $C_6As_3H_9$ phases should be close to 1079.7 J·K^{-1}·mol^{-1} and 953.4 J·K^{-1}·mol^{-1}, respectively. Interestingly, Baquerizo *et al.* did attempt to find a zero-hysteresis curve for Eq. 9 and Eq. 10 which might represent the true equilibrium. They used the curve to calculate an alternative standard entropy for $C_6As_3H_{13}$ and found it to be 1132.5 J·K^{-1}·mol^{-1}. This is in fact quite close to the value of 1079.7 J·K^{-1}·mol^{-1} estimated from the volume-based method here. This is an important outcome, as it indirectly confirms the validity of the zero-hysteresis approach chosen by Baquerizo *et al.* [32] in order to define the equilibrium properties of meta-ettringite. Nevertheless, for reasons not discussed in [3], the zero hysteresis data are currently not included in *Cemdata18*.

3.1.2 tricarboaluminate

According to Fig. 3, it also seems that the data point for $C_6Ac_3H_{32}$ lies slightly above Eq. 6. Although the difference seems small on the scale of the graph, it is around 150 J·K^{-1}·mol^{-1}, which is significant and beyond the uncertainty level of Eq. 6 [25]. It is known that $C_6Ac_3H_{32}$ is metastable with respect to

C_4AcH_{11}; thus, studies have paid less attention to the thermodynamic properties of $C_6Ac_3H_{32}$ [9,10]. For instance, *Thermoddem* includes no thermodynamic data for this phase. Nevertheless, Matschei *et al.* [22] estimated the standard entropy of $C_6Ac_3H_{32}$, which is used in [3], by employing the reference reaction in Eq. 15:

$$C_6Ac_3H_{32} + 3Cc \rightarrow C_6As_3H_{32} + 3Cs \quad (15)$$

where $\Delta_r S^\circ$ is assumed to be zero and the standard entropies of $C_6As_3H_{32}$, Cc and Cs are 1900 $J \cdot K^{-1} \cdot mol^{-1}$, 93 $J \cdot K^{-1} \cdot mol^{-1}$ and 107 $J \cdot K^{-1} \cdot mol^{-1}$, respectively. This led to a standard entropy of 1858 $J \cdot K^{-1} \cdot mol^{-1}$ for $C_6Ac_3H_{32}$. A possible reason for the observed discrepancy might reside in the value of molar volume given for this phase in [3] being inconsistent with the hydration level of $32H_2O$. That molar volume was calculated by Thomas *et al.* [22] using the unit cell parameters given in Taylor's book [34]. To test this hypothesis, we use Eq. 15 but replace $C_6Ac_3H_{32}$ and $C_6As_3H_{32}$ by their $30H_2O$ water content counterparts. Taking 1792.4 $J.K^{-1}.mol^{-1}$ as the standard entropy of $C_6As_3H_{30}$ (reported in [3] for this phase), the standard entropy of $C_6Ac_3H_{30}$ would be 1750.4 $J \cdot K^{-1} \cdot mol^{-1}$ which is closer to the estimate from Eq. 6 (1709.7 $J \cdot K^{-1} \cdot mol^{-1}$). Nevertheless, the exact reason for the observed inconsistency is not easy to identify at this stage, as the water contents of carbonate AFt phases are still subject to some uncertainty.

3.1.3 thaumasite

Another hydrate that is worthwhile to discuss here is thaumasite. Two values have been reported for the standard entropy of thaumasite, but they differ by about 40 $J \cdot K^{-1} \cdot mol^{-1}$. *Cemdata* [3] reports 897.1 $J \cdot K^{-1} \cdot mol^{-1}$, whereas Blanc *et al.* gave 941.5 $J \cdot K^{-1} \cdot mol^{-1}$ [10] although the molar volumes are identical in both compilations. The former value, shown in Fig. 3, agrees well with Eq. 6, and it was originally calculated by Matschei *et al.* [35] using the solubility products of phase-pure thaumasite measured at several temperatures. On the other hand, Blanc *et al.* [10] approximated the entropy following the method used by Schmidt *et al.* [36], assuming a fictive reaction with $\Delta_r S^\circ = 0$ involving seven compounds of known entropies (including amorphous SiO_2). However, as discussed earlier, the assumption of $\Delta_r S^\circ = 0$ should be used with high caution, as this method is susceptible to errors propagation depending on the type and number of compounds chosen. The reference reaction proposed by Schmidt *et al.* [36] is rather long with an unusually high number of compounds, making it even more prone to errors. Since the value obtained by Matschei *et al.* [35] is more consistent with Eq. 6, it seems reasonable to infer that their value is more accurate, compared to that proposed in *Thermoddem* [10].

3.2 Layered double hydroxides: AFm phases and hydrotalcite

Figure 5 shows the extent to which the standard molar entropies and formula unit volumes of AFm phases included in *Cemdata* [3] can be described by Eq. 6. All phases appear to match the linear trend, although slight deviations from Eq. 6 can be seen. All data points of C_4AH_n lie above Eq. 6 with some of the entropy values exceeding Eq. 6 by as much as 100 $J \cdot K^{-1} \cdot mol^{-1}$. Some of the M_xAH_n phases seem to have been underestimated, compared to Eq. 6.

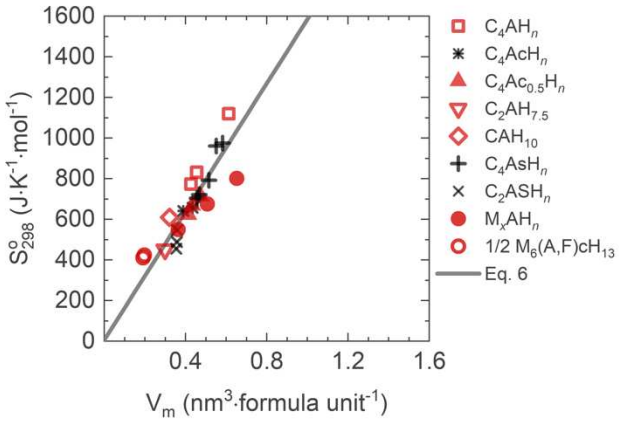

Fig. 5: Standard molar entropy versus formula unit volume of several AFm hydrates and M_xAH_n phases. Entropies are from [3]. Formula unit volumes were calculated using Eq. 5, using the molar volumes tabulated for these phases in Tables 1 and 3 of [3]. The solid line represents Eq. 6. Subscript *n* denotes water content, and *x* is the M/A ratio; here *x* can be 4, 6 or 8.

3.2.1 C_4AH_n

With respect to C_4AH_n phases, Lothenbach *et al.* [37] calculated the standard entropy of C_4AH_{19} using the solubility product of this phase reported in the literature. To do this, the authors fitted a three-term approximation to the temperature dependence of the solubility product, Eq. 16, using experimental solubility data:

$$\log K_T = 0.4343R^{-1}.(A_0 - A_2T^{-1} + A_3 \ln T), \quad (16)$$

where K_T is the solubility product at temperature T, and A_0, A_2 and A_3 are;

$$A_0 = \Delta_r S^\circ_{298} - \Delta_r C_p{}^\circ_{298}(1 + \ln T_0) \quad (17)$$

$$A_2 = \Delta_r H^\circ_{298} - \Delta_r C_p{}^\circ_{298} T_0 \quad (18)$$

$$A_3 = \Delta_r C_p{}^\circ_{298} \quad (19)$$

where T_0 is 298.15 K, and $\Delta_r S^\circ_{298}$, $\Delta_r C_p{}^\circ_{298}$ and $\Delta_r H^\circ_{298}$ represent the change of entropy, heat capacity and enthalpy of reaction, respectively, at standard temperature of 298.15 K. Considering Eq. 20 which represents the formation of C_4AH_{19}, the standard entropy of C_4AH_{19} can be deduced by fitting Eq. 16 to the measured solubility products.

$$C_4AH_{19} \rightarrow 4Ca^{2+} + 2Al(OH)_4^- + 6OH^- + 12H_2O, \quad (20)$$

To fit Eq. 16 to the solubility products measured at different temperatures, the value of $\Delta_r S^\circ_{298}$ in Eq. 20 has to be adjusted by changing only the standard entropy of C_4AH_{19}, as the standard entropies of the ions and water in Eq. 20 are known.

A reason for the discrepancy observed between Eq. 6 and the C_4AH_{19} data point in Fig. 5 could be that the solubility data gathered from the literature by Lothenbach *et al.* [37] were inaccurate or misleading. It is important to note that C_4AH_{19} is metastable with respect to C_3AH_6 and CH at 20 ºC and higher temperatures. Although the authors of [37] were careful of this phenomenon and chose solubility data of samples that had been reacted for more than 10 months at temperatures below 20 ºC, it might have still been the case that the very old samples had started to decompose to C_3AH_6 and CH or were subject to carbonation. It follows that fitting Eq. 12 to those data would have led to propagation of errors. If so, these errors would also have carried over into the entropy data for C_4AH_{11} and/or C_4AH_{13}, which were calculated from that of C_4AH_{19} by Baquerizo *et al.* [38] using the same method they used for ettringite (as outlined in Section 3.1) but with reactions Eq. 21 and Eq. 22 instead:

$$C_4AH_{11} + 2H_2O \rightarrow C_4AH_{13} \quad (21)$$

$$C_4AH_{13} + 6H_2O \rightarrow C_4AH_{19} \quad (22)$$

Alternatively, the standard heat capacity of C_4AH_{19} might be the origin of error since heat capacity is a key parameter involved in the fitting equations (*i.e.* Eq. 18 and Eq. 19). Nevertheless, it is difficult to verify this hypothesis without newly measured heat capacity data.

3.2.2 M_xAH_n

Regarding the M_xAH_n solid solutions, Myers *et al.* [21] estimated the standard entropies of M_4AH_{10}, M_6AH_{12} and M_8AH_{14} by adjusting the standard entropy of $Mg_{0.74}Al_{0.26}(OH)_2(CO_3)_{0.13}{\cdot}0.39H_2O$ using the additivity method (Eq. 1), with $Mg(OH)_2$ and $MgCO_3$ as constituents. For example, Eq. 23 shows how to build up the standard entropy of M_4AH_{10}:

$$S^\circ_{M_4AH_{10}} = 2\left(\frac{1}{0.26} S^\circ_{Mg_{0.74}Al_{0.26}(OH)_2(CO_3)_{0.13}\cdot 0.39H_2O} - 0.5 S^\circ_{MgCO_3} - 0.346 S^\circ_{Mg(OH)_2}\right) \quad (23)$$

Equation 6 almost fits the standard entropy of M_4AH_{10}, as shown in Fig. 5, but this is not the case for M_6AH_{12} and M_8AH_{14}. There could be two reasons for this; either the molar volumes for these two phases are not accurately reported in the datasets used [3,21], or errors in the standard entropies of compounds used in Eq. 23 have led to the underestimation of entropy.

The first could be unlikely. The molar volumes reported for M_xAH_n in [3,21] were based on the theoretical estimations according to the model outlined by Richardson in [39,40]. Richardson's model is based on a set of experimental data and is carefully formulated by taking into account how the crystal lattice parameters change when a fraction of trivalent cations replaces divalent cations in M_xAH_n. Therefore, this leaves little doubt that the molar volumes calculated by Myers *et al.* [21] according to Richardson's model are relatively accurate.

The errors arising from the value of standard entropies used in Eq. 23 could also be improbable. The standard entropies of magnesium carbonate and hydroxide are known to high precision, and Myers *et al.* [21] adopted the standard entropy of $Mg_{0.74}Al_{0.26}(OH)_2(CO_3)_{0.13}{\cdot}0.39H_2O$ from [41] where the authors determined entropy by using the third law and low-temperature heat capacity measurements. Although it is not easy to verify the accuracy of their heat capacity data, it is sensible to assume that the derived standard entropy for this phase is sufficiently reliable, in particular that the standard entropy and volume of M_4AH_{10} is in agreement with Eq. 6.

In spite of the above, the observed inconsistencies could be due to the choice of compounds used in Eq. 23. To test this hypothesis, the standard entropies of M_xAH_n is recalculated here but with a different fictive reaction than that in Eq. 23. To that end, it is useful to revisit the chemical formula and structural constituents of layered double hydroxides, as given in Eq. 24:

$$\left[\mathrm{M}^{2+}_{(1-x')}\mathrm{M}^{3+}_{x'}(\mathrm{OH})_2\right](\mathrm{A}^{n'-})_{\frac{x'}{n'}}\cdot m'\mathrm{H_2O} \qquad (24)$$

where M^{2+} and M^{3+} are divalent and trivalent cations. If the ratio of cations (M^{2+}/M^{3+})=Q, then x'=$1/(1+Q)$. $A^{n'-}$ is the anion (*e.g.* OH^-) in the interlayer region and m' is the number of water molecules per cation. Hence, for one main layer of M_8AH_{14}; Q=4, x'=1/5, n'=1 and m'=3/10. The structure of the cation layer in M_xAH_n phases consists of a series of edge-sharing octahedra where cations M^{2+} and M^{3+} are distributed with a particular order depending on the x' value. A portion of hydroxyl groups are part of octahedra, with the rest being in the form of hydroxyl ions in the interlayer region to balance the extra electrostatic charge resulting from M^{2+} substitution by M^{3+}. With this in mind, it might make more sense to write the standard entropy of M_xAH_n in Eq. 23 as an additive quantity of $Mg(OH)_2$, $Al(OH)_3$ and H_2O entropies, as in principle these hydroxides and water are the main constituents of M_xAH_n. In this way, the estimated entropy could be more consistent with M_xAH_n crystal structure. Therefore, for M_8AH_{14} for which the highest discrepancy was observed in Fig. 5, one may write:

$$\mathrm{S^\circ_{M_8AH_{14}}} = 2x'\mathrm{S^\circ_{Mg(OH)_2}} + 2\mathrm{S^\circ_{Al(OH)_3}} + 3\mathrm{S^\circ_{H_2O}};\ x'=4 \qquad (25)$$

where the standard entropies of $Mg(OH)_2$, $Al(OH)_3$ and H_2O are assumed to be 63.1 $J{\cdot}K^{-1}{\cdot}mol^{-1}$, 140 $J{\cdot}K^{-1}{\cdot}mol^{-1}$ (taken from Table 1 in [21]) and 69.92

490 J·K^{-1}·mol^{-1} (Table D1 in [3]). This gives $S^{\circ}_{M_8AH_{14}}$=994.65 J·K^{-1}·mol^{-1} which is
491 close to the estimation from Eq. 6; *i.e.* 1034.9 J·K^{-1}·mol^{-1}.

492 An important issue worth discussing regarding Eq. 25 is the choice of entropy
493 value for $Al(OH)_3$. The standard entropy value used above for this hydroxide
494 is for the so-called microcrystalline $Al(OH)_3$. This phase is less crystalline
495 than gibbsite and so has a higher standard entropy [42]. It turns out that in
496 order to reach the same value of entropy for M_4AH_{10} as Eq. 23 (and to ensure
497 that the M_4AH_{10} data point matches Eq. 6 with the molar volume calculated
498 in [21]), $S^{\circ}_{Al(OH)_3}$ in Eq. 25 should be adjusted to that of gibbsite (*i.e.* 70 J·K^{-1}·mol^{-1} [22]). This gives $S^{\circ}_{M_4AH_{10}}$= 602.2 J·K^{-1}·mol^{-1} which is near 549 J·K^{-1}·mol^{-1} estimated with Eq. 23. Blanc *et al.* [10] also estimates an intermediate
501 value of 552 J·K^{-1}·mol^{-1} using similar compounds as those in Eq. 23 although
502 they make no estimates for higher *x'* values, and so it is not possible to make
503 direct comparison for those phases. The fact that $S^{\circ}_{Al(OH)_3}$ value needs to be
504 changed depending on *x'* might well be due to the change of Al^{3+} state in the
505 crystal structure of M_4AH_{10} compared to M_8AH_{14}; this could be an interesting
506 area of future research.

507 These findings and the variation of estimations from different fictive reactions
508 prove that the *additivity method* is sensitive to the selection of constituents
509 and that in cases this may lead to inconsistent estimations. To avoid these,
510 it would be useful if future studies measure the standard entropy of M_xAH_n
511 phases using the third law and heat-capacity measurements.

512

513 3.3 Fe-bearing phases

514 The standard molar entropies of all iron-bearing phases included in [3] are
515 presented in Fig. 6, along with their formula unit volumes. Somewhat
516 surprisingly, the data points of only two of these ten phases are in reasonable
517 agreement with Eq. 6; these are Fe-ettringite ($C_6Fs_3H_{32}$) and C_4FH_{13}.

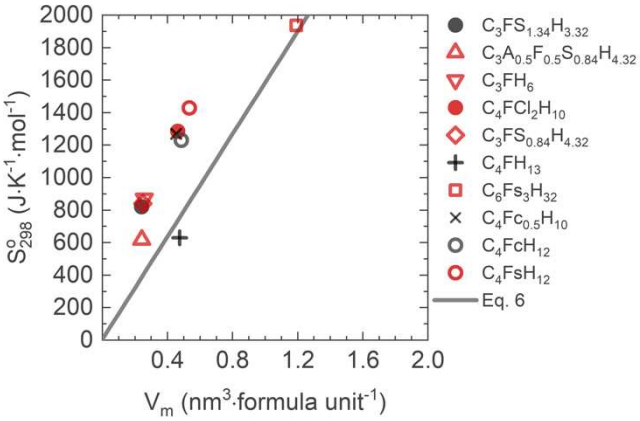

Fig. 6: Standard molar entropy versus formula unit volume of several Fe-bearing hydrates. Entropies are from [3]. Formula unit volumes were calculated using Eq. 5 and the molar volumes tabulated for these phases in Table 1 of [3]. The solid line represents Eq. 6.

Möschner *et al.* [43] estimated the standard entropy of Fe-ettringite using Eq. 26 and the assumption that $\Delta_r S^{\circ}=0$ for this reaction:

$$C_6Fs_3H_{32} + A \rightarrow C_6As_3H_{32} + F \quad (26)$$

where the major hydrate with a similar structure to Fe-ettringite is Al-ettringite which was shown earlier (Fig. 3) to be well described by Eq. 6. Therefore, it comes as no surprise that Fe-ettringite is also consistent with Eq. 6.

The data point shown for C_4FH_{13} in Fig. 6 lies slightly below the prediction of Eq. 6. Dilnesa *et al.* [44] derived the standard entropy of this phase by fitting Eq. 12 to its solubility products measured experimentally at temperatures of 20 and 50 °C. The use of Eq. 12 has caused the underestimation of the standard entropy by about 100 J·K^{-1}·mol^{-1}. Two factors could have been at the origin of this discrepancy, which is worthy of discussion although less marked than in the case of some of the other Fe-bearing hydrates. First, the authors of [44] measured the solubility product of C_4FH_{13} at 20 °C for samples which were left to react for one or two years; however, in the case of the 50 °C samples, they were kept for seven days only which might have been insufficient for reaching equilibrium conditions. Second, some uncertainty could be associated with the fitting of Eq. 12 to the measured data since only two temperatures were studied.

The rest of the data points shown in Fig. 6 are related to several AFm and hydrogarnet phases, containing Fe^{3+} isomorphously substituted for Al^{3+}. As for C_4FH_{13}, the entropy of these phases were all derived experimentally by Dilnesa *et al.* via Eq. 16 and solubility measurements [44–47]. There are no other data reported for these hydrates to allow for direct comparison between studies, except for C_4FsH_{12}. Dilnesa *et al.* [46] derived the standard entropy of C_4FsH_{12} and found it to be 1430 J·K^{-1}·mol^{-1}. This value lies markedly above Eq. 6 (provided that there are no errors associated with the molar volume of

549 this phase reported in [3], but this should be unlikely as the molar volume
550 reported for C_4FsH_{12} is quite close to that of C_4AsH_{12}). This value disagrees
551 with 833 $J{\cdot}K^{-1}{\cdot}mol^{-1}$ that was estimated theoretically by Blanc *et al.* [10] using
552 a reference reaction based on isomorphous Fe/Al substitution into C_4AsH_{12}
553 and the assumption that $\Delta_r S^\circ=0$. Their estimated value is much closer to the
554 prediction of Eq. 6 (*i.e.* 842.4 $J{\cdot}K^{-1}{\cdot}mol^{-1}$).

555 It is difficult at this stage to identify the exact cause of large discrepancies
556 between the Eq. 6 trend and the studies of Dilnesa *et al.*, and this certainly
557 requires further experimental investigation. Since Dilnesa *et al.* relied on
558 solubility data to calculate the standard entropy, there may be uncertainty in
559 the solubility products measured for these phases, *e.g.* some influence of
560 unreacted C_2F which was employed as the starting material but persisted in
561 the samples after a long reaction time. This is an important finding and needs
562 attention, especially as commonly-used cements (such as Portland cement)
563 may contain more quantities of iron-bearing phases in the future [48].

564 It should be mentioned that the presence of iron in minerals causes magnetic
565 disorder, which is known to affect the heat capacity and so standard entropy.
566 However, the extent of such changes is expected to be in the order of few
567 entropy units only [16,17], but the discrepancies observed in Fig. 6 are as
568 high as 600 $J{\cdot}K^{-1}{\cdot}mol^{-1}$. Therefore, it is highly unlikely that the magnetic effect
569 of iron is the reason why the entropy data for iron-bearing phases are so
570 deviated from Eq. 6.

571

572 3.4 Hydrates with varying water content

573 From the preceding discussion, it is clear that the estimation of the standard
574 entropies of hydrates with varying water content has in many cases been
575 problematic. Here, we employ Eq. 8, which was originally developed for ionic
576 hydrates only, to examine whether it is suitable to apply it to cement-related
577 hydrates. However, the key issue that needs attention is the state of water
578 molecules in hydrated crystals. Overall, the bonding state of water with the
579 crystal lattice constituents can affect the lattice vibration modes and hence
580 the standard heat capacity and entropy of the crystal. In general, water can
581 occur in three forms in cement hydrates: (i) crystal water, in which water is in
582 the form of OH; (ii) coordination water, in which water molecules are bound
583 to the constituents of the lattice; or (iii) zeolitic water, in which water
584 molecules are not bound to the lattice, but fill in the vacancies only. In the
585 original derivation of Eq. 8, the constant m refers to the coordination water
586 only, given that the hydrates studied by Jenkins and Glasser [31] contained
587 this form of water in their structures. With respect to the thermodynamic
588 modelling of cements, hydrates involving in reactions whereby crystal water
589 is removed are not of interest, as dehydroxylation to such an extent would
590 transform the hydrate to a completely different compound. Therefore, we

propose that it suffices to use Eq. 8 as long as the change of water content concerns the coordination (and zeolitic) water state.

Fig. 7 compares points calculated using Eq. 8, in which the value of $\theta_{S^\circ_{298}}$ is 40.9 $J \cdot K^{-1} \cdot mol^{-1} \cdot (H_2O \text{ molecule})^{-1}$ [31], against the gradient of standard entropies (as a function of water content) for several AFt, AFm and hydrogarnet phases: C_6AsH_m, C_4AsH_m, C_2ASH_m (or $C_4A(AS_2)H_m$), C_4AH_m and $C_4Ac_{0.5}H_m$ where η in Fig. 7 denotes the number of water molecules in coordination and zeolitic states. All gradients are presented as a function of η, which was calculated by subtracting the number of bound hydroxyl groups in the hydrate structure from the total number *m* of water molecules in the formula of each crystal. The number of bound hydroxyls for C_6AsH_m, C_4AsH_m, $C_4A(AS_2)H_m$, C_4AH_m and $C_4Ac_{0.5}H_m$ are 6, 6, 5, 7, and 7 respectively, according to the structures described in [32,38,49]. All standard entropies used in Fig. 7 are based on experimental derivations and fit the entropy-volume relationship in Fig. 3 or Fig. 5. The standard entropies of $C_6As_3H_9$ and $C_6As_3H_{13}$ derived experimentally in [32] are not shown in Fig. 7, as they are for non-equilibrium conditions.

It can be seen from Fig. 7 that all calculated gradients follow Eq. 8 although there are slight deviations from the linear trend. This could be due to the possible errors in the correlation of entropy data from one hydration state to another, but the striking observation is that if the value of *m* is correctly selected based on crystal chemistry, it is possible to predict and/or compare the standard entropies at different hydration levels. Our finding here further reinforces the estimation method proposed by Jenkins and Glasser [29,31].

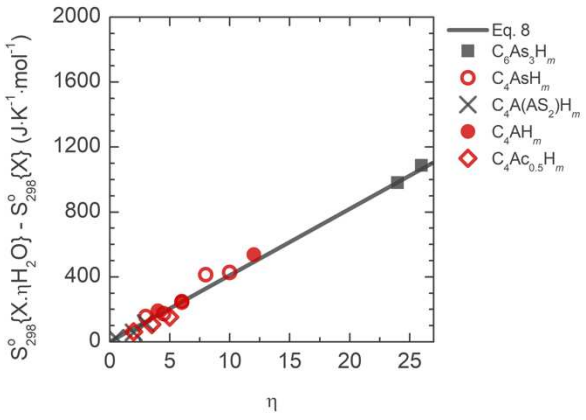

Fig. 7: Gradient of standard entropies (based on the definition in Eq. 8) as a function of the number η of molecular (coordination or zeolitic) waters per formula unit, shown for several AFt, AFm and hydrogarnet phases. The entropy values of $C_6As_3H_9$ and $C_6As_3H_{13}$ are not included here, as they are for non-equilibrium conditions.

3.5 Silicate hydrate solid solutions

Figure 8 shows the standard molar entropies and formula unit volumes of solid solution models used in [3] to describe some of the alkali-earth silicate hydrates forming during the hydration of Portland and other cements. It is immediately evident that many of the data points are not well described by Eq. 6.

The data points for CSH-II are inconsistent with Eq. 6. The standard entropy of the CSH-II model originates from [9] where the authors used solubility data to calculate entropy, and estimated ±50 $J \cdot K^{-1} \cdot mol^{-1}$ uncertainty in their values; this is, to a degree, consistent with the observations from Fig. 8.

All ECSH-1 and ECSH-2 phases from [50,51] are well described by Eq. 6, except for $C_{0.83}SH_{1.83}$, $CS_{0.6}H_{1.1}$ and $SrSH_2$. The standard entropy data for these phases were developed in [50,51] where the authors used the additivity method of Eq. 1 (with constituents being in the form of oxide and water) and molar volumes were derived using gram-formula masses and an assumed dry bulk density; any of which could be the source of the discrepancy of these data from Eq. 6. It should be noted that the accurate determination of water contents and molar volumes of specific hydrous silicates is complex and still prone to significant uncertainty.

For CSHQ, CNASH and CSH3T models of silicate hydrates, there are points that are far below Eq. 6. The reasons for these are also not easy to identify, as both the standard entropies and molar volumes were estimated in the reference studies [20,52]; these are the end-members of thermodynamic models for complex solid solutions, and so in general they were not actually synthesised as pure phases in any of those studies. If the source of error is the molar volume of any given end-member, then this needs immediate attention as the change of volume as a result of formation or decomposition of silicate hydrates can influence the porosity and durability of cementitious materials containing these hydrates.

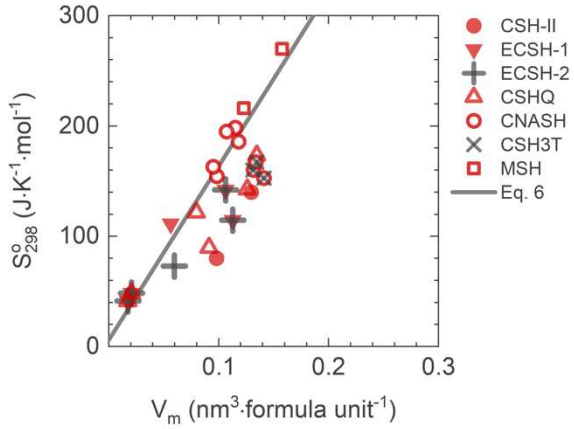

Fig. 8: Standard molar entropy versus formula unit volume of a variety of alkali-earth silicate hydrate solid solutions. Entropies were retrieved from [3], but they were originally calculated in [9], [20], [51], [50], [52], and [53]. Formula unit volumes were calculated using Eq. 5 and the molar volumes given in Table 1 of [3]. The solid line represents Eq. 6.

3.5 Zeolites

For zeolites included in *Cemdata18* [3], which are zeolite P(Ca), natrolite, chabazite, zeolite X(Na) and zeolite Y(Na), all appear to be well described by Eq. 6 apart from zeolite P(Ca) (see Fig. 9), which is somewhat controversial. In the *Thermoddem* database, the standard entropy of zeolite P(Ca) is 397 J.K^{-1}.mol^{-1} which is much closer to Eq. 6 (407 J.K^{-1}.mol^{-1} with V_{molar}=153 cm^3.mol^{-1}), compared to 779 J.K^{-1}.mol^{-1} in *Cemdata18* which was derived originally by Lothenbach *et al.* in [54]. In both cases, the authors used the solubility product at various temperatures to calculate the standard entropy, and there is a clear difference between the solubility data measured by Lothenbach *et al.* in [54] and those reported by Blanc *et al.* [55]. Therefore, it is reasonable to suggest that the origin of the discrepancy lies in the measured solubility data.

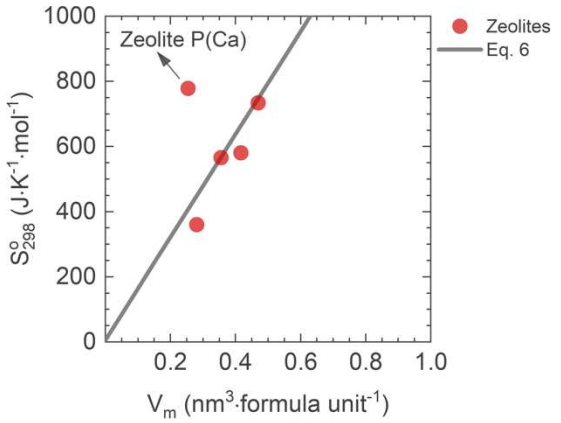

Fig. 9: Standard molar entropy versus formula unit volume of several zeolites. Entropies and the molar volumes are from [3]. Formula unit volumes were calculated using Eq. 5. The solid line represents Eq. 6.

4. Clinker minerals

Figure 10 shows the standard molar entropies of clinker minerals (given in [3]) as a function of their formula unit volumes. The dashed line represents Eq. 7, which evidently fits the entropy and volume data very well. This finding was somewhat expected, as the entropy data of most of the clinker minerals come from the same standard database as was used by Jenkins and Glasser [25] to develop their equation. As highlighted earlier, caution must be taken when Eq. 7 is used for modelling different polymorphs of the same mineral, as it is possible that standard entropy is not an increasing function of formula unit volume; an example of this was given in Section 2. Nevertheless, Eq. 7 is useful to provisionally estimate the standard entropy of some of the clinker minerals for which thermodynamic data are scarce, such as ye'elimite and ternesite.

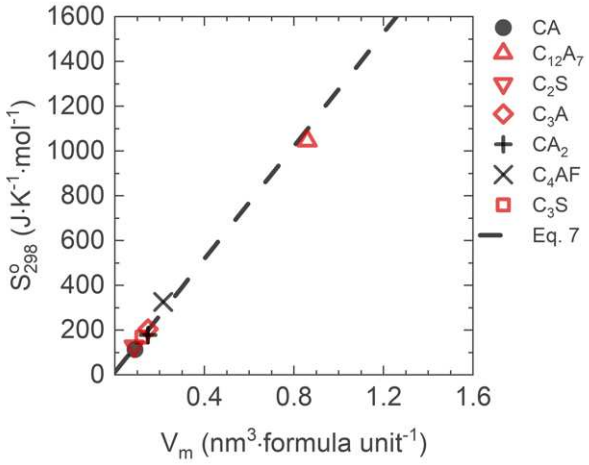

Fig. 10: Standard molar entropy versus formula unit volume of clinker minerals. Entropies are from [3]. Formula unit volumes were calculated using Eq. 5 and the molar volumes tabulated for the clinker minerals in Table 1 of [3]. The dashed line represents Eq. 7. Note that it is unclear in [3] what polymorphs these minerals are, and as a result this detail is missing here.

4.1 Standard entropy of ye'elimite and ternesite

Entropy data for ye'elimite and ternesite are scarce in the literature. Hanein *et al.* [2,56,57] derived entropy data of these minerals at high temperatures from existing vapour pressure measurements, but there is not sufficient data to accurately extrapolate these down to 298.15 K. Eq. 7 can be helpful here. The standard entropies of different polymorphs of ye'elimite and ternesite are estimated and shown in Table 1, using Eq. 7 and their unit cell volumes from [58–60]. Unit cell volume was converted to formula unit volume via Eq. 27:

$$\mathrm{V_m} = \frac{\mathrm{V}_{cell}}{1000\ \mathrm{Z}} \tag{27}$$

where V_{cell} is unit cell volume in Å^3 and Z is the number of formula units within the crystallographic unit cell. The estimated entropy values in Table 1 should be verified with careful experimental techniques in the future, but these data can serve as provisional estimates. We attempted to test the accuracy of the entropy value for ye'elimite (see Appendix A for more detail), and it appears to be in reasonable agreement with Table 1.

Table 1: Estimated standard molar entropy of orthorhombic ye'elimite (Pcc2) and cubic ye'elimite (I43m) and ternesite using Eq. 7

Crystal name (symmetry group)	V_{cell} (Å^3)	Z	Reference study	V_m (nm^3)	$S°_{298}$ (J·K^{-1}·mol^{-1}) estimated
Ye'elimite (Pcc2)	1557.78	4	[58]	0.389	504.5
Ye'elimite (I43m)	789.55	2	[60]	0.394	511.2
Ternesite (Pnma)	1075.12	4	[59]	0.268	352.2

5. Conclusions

Methods to estimate the standard entropy of cement hydrates or clinker minerals are useful for the purpose of thermodynamic modelling, especially to assess the quality of existing entropy data obtained via experiments. This study employed a simple mathematical relationship, established by Jenkins and Glasser [25], to examine the accuracy of standard entropies and molar volumes of cement related substances listed in established thermodynamic datasets for cements. The relationship used here relates the standard molar entropy of an inorganic solid to its formula unit volume via a linear equation with known constants.

In general, the standard entropies and molar volumes of many cement hydrates were found to be consistent with Jenkin and Glasser's relationship. The exceptions to this were:

- two ettringite-group phases with water contents of 9 and 13H_2O
- magnesium/aluminium layered double hydroxide solid solutions
- almost all Fe-bearing monosulfate and hydrogarnet phases, and
- several calcium silicate hydrate end-members.

The entropy data for some of these phases were derived in previous studies by measuring the solubility products at different temperatures and fitting the three-term approximation equation of solubility product to those measured solubility data. The fitting equation is a function of standard entropy, and to achieve a desired fitting, the entropy term is the key parameter that needs to be adjusted. In view of this, errors associated with standard entropies can imply inaccuracies in solubility product measurements. Thus, there are now open questions as to whether the measured solubility products for some of the phases listed above are reliable. This deserves closer investigation, especially given that the formation or decomposition of most of these phases have important implications for modelling the dimensional stability and/or durability of cement systems.

The standard entropies for clinker minerals were found to linearly correlate to their formula unit volumes, consistent with Jenkins and Glasser's equation. The standard entropy of clinker minerals ye'elimite and ternesite were also estimated provisionally using the volume-based relationship.

Acknowledgements

The authors would like to thank Prof. Fredrik Glasser and Dr. Isabel Galan for providing the ye'elimite sample and XRD analyses. The authors would also like to thank Dr. Stefan Schmölzer and Peter Davies from NETZSCH Gerätebau GmbH who conducted the heat capacity measurements on the ye'elimite sample.

Appendix A.

The standard entropy of ye'elimite was experimentally derived using its heat capacity over a range of temperatures and the third law (Eq. 28).

$$S°_{298} = \int_{0}^{298.15} \frac{Cp}{T} dt \quad (28)$$

A.1 synthesis of ye'elimite

Ye'elimite was synthesised by sintering the stoichiometric mixture of Al_2O_3, $CaSO_4$ and $CaCO_3$ (Sigma-Aldrich, ACS reagent, ≥99%). The reagents were first mixed for five minutes using a mortar and pestle. A few drops of ethanol were also added to the mix to facilitate mixing. The reagents were then left in an oven set at 100 °C for 2 hours to dry. Once the required time had elapsed, the dried mixture was placed into a platinum crucible and subjected to heating at 1250 °C for a period of 20 minutes in a muffle furnace. Thereafter, the sample was removed from the furnace and quenched at room temperature. The sample was then homogenised using the mortar and pestle and placed again into the furnace. This process was repeated five times until the resultant material was highly pure ye'elimite. To confirm the purity, X-ray diffraction pattern of the sample was recorded over 2θ ranging from 5° to 70° with a step size of 0.026° using a Philips Empyrean diffractometer operated at 45 kV and 40 mA. The source of X-ray was Cu Kα, and the diffractometer was equipped with a Ge monochromator and a PIXcel1D detector. The sample holder was set to rotate at 15 rpm to improve counting statistics. Fig. A.1 shows the X-ray powder diffraction pattern measured for the ye'elimite sample. The result of Rietveld analysis (carried out using GSAS software) indicates that the sample is primarily composed of about 97% ye'elimite with slight trace of Cs and CA.

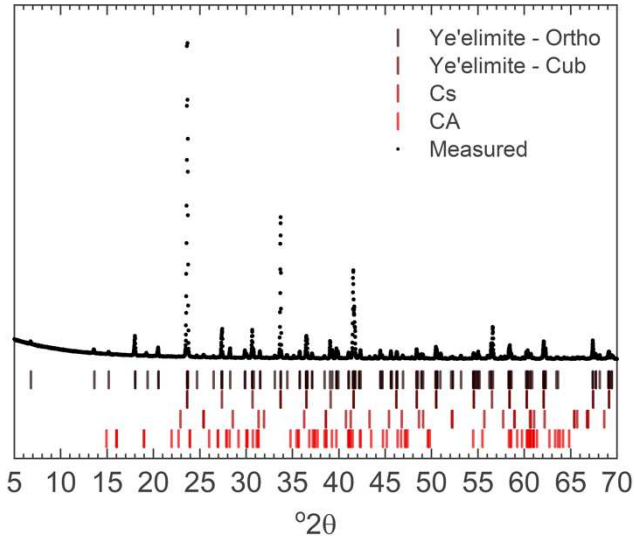

Fig. A.1: Measured X-ray powder diffraction pattern of synthesised ye'elimite (shown with dots), indicating the presence of cubic and orthorhombic polymorphs of ye'elimite (based on [58] and [60], respectively) as well as a slight trace of Cs (ICSD 16382) [61] and CA (ICSD 602) [62]. The ICSD database search was based on the recommendations given in [63]. The Rietveld analysis suggests the following composition: 87.1% orthorhombic and 9.4% cubic ye'elimite, 0.8% Cs and 2.7% CA (wRp = 8.72).

A.2 heat capacity measurements of ye'elimite

The heat capacity of ye'elimite was measured using a differential scanning calorimeter (DSC 214 Polyma, NETZSCH) and based on ASTM E1269 [64]. Measurements were conducted in duplicates on 20±0.1 mg sample placed in a closed alumina crucible. The sample was cooled down to -170 °C using liquid nitrogen cooling, then kept at a 10-min isotherm and heated up to 30 °C at 10 K/min. Ideally, the heat capacity should have been measured from temperatures starting from near 0 K in order to ensure that the behaviour of the material is captured at low temperatures. However, this was not possible with the available resources in this study; thus, the value calculated here is expected to deviate from its true value. To assess whether deviation due to the measurement technique occurred, the heat capacity of K_2CO_3 (ACS reagent, 99%) was also measured as a control.

The measured heat capacity patterns were fitted by a combination of Debye and Einstein functions, given by Eq. 29, which are shown to well describe the heat capacity of solids at temperatures below 300 K [65,66]. The resultant fitting function was then used in Eq. 28 to calculate standard entropy. Here it is assumed that the isobaric and isochoric heat capacities are the same; *i.e.*, volume remains constant throughout the measurements. This assumption is valid in the temperature range studied in this paper [16].

$$C_p = mD\left(\frac{\theta_D}{T}\right) + nE\left(\frac{\theta_E}{T}\right) \quad (29)$$

$$D\left(\frac{\theta_D}{T}\right) = 9R\left(\frac{T}{\theta_D}\right)^3 \int_0^{\frac{\theta_D}{T}} y^4 \frac{e^y}{[e^y - 1]^2} dy \quad (30)$$

$$E\left(\frac{\theta_E}{T}\right) = 3R\left(\frac{\theta_E}{T}\right)^2 \frac{e^{\frac{\theta_E}{T}}}{\left[e^{\frac{\theta_E}{T}} - 1\right]^2} \quad (31)$$

For Eqs. 29-31, m, n, θ_D and θ_E are the fitting parameters. R is the universal gas constant and T is the temperature in Kelvin. To fit Eq. 29 to the measured data, an algorithm was written in MATLAB incorporating a least-square fitting function. The measured data were fitted from 120 K to 300 K. We chose this range of temperatures as it was noted that the heat capacity data below 120 K were abnormal and inconsistent with those known for K_2CO_3. As a general rule, the sum of m and n parameters obtained from the fitting process ought to be equal to the number of atoms in the compound's formula [65,66]. For example, $m + n$ =6 for K_2CO_3.

The measured and fitted heat capacity patterns for ye'elimite and K_2CO_3 are shown in Fig. A.2. There are no anomalies in the measured data for K_2CO_3 within the temperature range presented here; however, ye'elimite pattern exhibits a feature around 273 K, which is attributed to the presence of water in the bulk material. This feature was removed from the fitting process by ignoring the measured data between 253 K and 285 K.

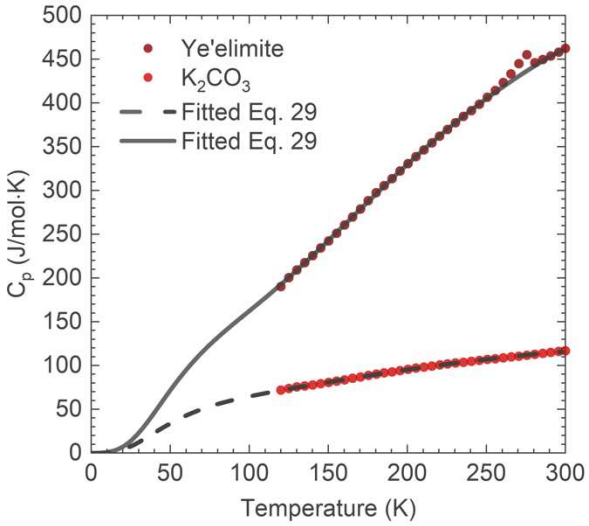

Fig. A.2: Measured (dots) and fitted (lines) heat capacity patterns of synthesised ye'elimite and K_2CO_3.

The fitting of K_2CO_3 heat capacity data results in a standard entropy of 147.28 $J.K^{-1}.mol^{-1}$ for this phase, with $m + n$ = 5.989. This value is reasonably consistent with 155.57 $J.K^{-1}.mol^{-1}$ known for this compound (≈5% deviation) [67]. In the case of ye'elimite sample, the standard entropy is found to be 432 $J.K^{-1}.mol^{-1}$ with $m + n$ = 27.05 (which is close to 27 atoms in its formula). This entropy value is close to the estimates given in Table 1, further validating Eq. 7. The discrepancy (≈15%; Pcc2; orthorhombic) is inevitable in the case of

our study because the ye'elimite sample contained impurities as well as two polymorphs, and that the heat capacity data below 120 K were lacking from the fitting process. In future studies, a purer sample needs be tested and other types of calorimetry (such as relaxation calorimetry where temperature can reach as low as near 0 K) may be employed to assess the accuracy of estimates in Table 1.

References

[1] T. Hanein, F.P. Glasser, M.N. Bannerman, Thermodynamic data for cement clinkering, Cem. Concr. Res. 132 (2020) 106043. https://doi.org/https://doi.org/10.1016/j.cemconres.2020.106043.

[2] T. Hanein, I. Galan, F.P. Glasser, S. Skalamprinos, A. Elhoweris, M.S. Imbabi, M.N. Bannerman, Stability of ternesite and the production at scale of ternesite-based clinkers, Cem. Concr. Res. 98 (2017) 91–100. https://doi.org/10.1016/j.cemconres.2017.04.010.

[3] B. Lothenbach, D.A. Kulik, T. Matschei, M. Balonis, L. Baquerizo, B. Dilnesa, G.D. Miron, R.J. Myers, Cemdata18: A chemical thermodynamic database for hydrated Portland cements and alkali-activated materials, Cem. Concr. Res. 115 (2019) 472–506. https://doi.org/10.1016/j.cemconres.2018.04.018.

[4] B. Lothenbach, M. Zajac, Application of thermodynamic modelling to hydrated cements, Cem. Concr. Res. 123 (2019) 105779. https://doi.org/10.1016/J.CEMCONRES.2019.105779.

[5] D.A. Kulik, T. Wagner, S.V. Dmytrieva, G. Kosakowski, F.F. Hingerl, K.V. Chudnenko, U.R. Berner, GEM-Selektor geochemical modeling package: Revised algorithm and GEMS3K numerical kernel for coupled simulation codes, Comput. Geosci. 17 (2013) 1–24. https://doi.org/10.1007/s10596-012-9310-6.

[6] T. Wagner, D.A. Kulik, F.F. Hingerl, S.V. Dmytrievava, Gem-selektor geochemical modeling package: TSolMod library and data interface for multicomponent phase models, Can. Mineral. 50 (2012) 1173–1195. https://doi.org/10.3749/canmin.50.5.1173.

[7] D. Parkhurst, C. Appelo, Description of Input and Examples for PHREEQC Version 3 - A Computer Program for Speciation, Batch-reaction, One-dimensional Transport, and Inverse Geochemical Calculations, in: U.S. Geol. Surv. Tech. Methods, B. 6, USGS, Denver, 2013: p. 497. https://doi.org/10.3133/tm6A43.

[8] B. Lothenbach, F. Winnefeld, Thermodynamic modelling of the hydration of Portland cement, Cem. Concr. Res. 36 (2006) 209–226. https://doi.org/10.1016/j.cemconres.2005.03.001.

[9] B. Lothenbach, T. Matschei, G. Möschner, F.P. Glasser, Thermodynamic modelling of the effect of temperature on the hydration and porosity of Portland cement, Cem. Concr. Res. 38

(2008) 1–18. https://doi.org/10.1016/j.cemconres.2007.08.017.

[10] P. Blanc, X. Bourbon, A. Lassin, E.C. Gaucher, Chemical model for cement-based materials: Thermodynamic data assessment for phases other than C-S-H, Cem. Concr. Res. 40 (2010) 1360–1374. https://doi.org/10.1016/j.cemconres.2010.04.003.

[11] P. Blanc, X. Bourbon, A. Lassin, E.C. Gaucher, Chemical model for cement-based materials: Temperature dependence of thermodynamic functions for nanocrystalline and crystalline C–S–H phases, Cem. Concr. Res. 40 (2010) 851–866. https://doi.org/10.1016/J.CEMCONRES.2009.12.004.

[12] T. Matschei, Thermodynamics of cement hydration, University of Aberdeen, 2007.

[13] F. Bellmann, J. Majzlan, K.D. Grevel, E. Dachs, H.M. Ludwig, Analysis of thermodynamic data of calcium aluminate monocarbonate hydrate, Cem. Concr. Res. 116 (2019) 89–94. https://doi.org/10.1016/j.cemconres.2018.10.012.

[14] T. Hanein, J.-L. Galvez-Martos, M.N. Bannerman, Carbon footprint of calcium sulfoaluminate clinker production, J. Clean. Prod. 172 (2018) 2278–2287. https://doi.org/10.1016/J.JCLEPRO.2017.11.183.

[15] V.I. Babushkin, G.M. Matveyev, O.P. Mchedlov-Petrossyan, Thermodynamics of silicates, Springer-Verlag, Berlin Heidelberg, 1985.

[16] Timothy J. B. Holland, Dependence of entropy on volume for silicate and oxide minerals: a review and predictive model, Am. Mineral. 74 (1989) 5–13.

[17] W.S. Fyfe, F.J. Turner, J. Verhoogen, Metamorphic reactions and metamorphic facies, The Geological Society of America, Baltimore, MD, 1958.

[18] B. Ransom, H.C. Helgeson, Estimation of the standard molal heat capacities, entropies and volumes of 2:1 clay minerals, Geochim. Cosmochim. Acta. 58 (1994) 4537–4547. https://doi.org/10.1016/0016-7037(94)90189-9.

[19] A. La Iglesia, J.. Félix, Estimation of thermodynamic properties of mineral carbonates at high and low temperatures from the sum of polyhedral contributions, Geochim. Cosmochim. Acta. 58 (1994) 3983–3991. https://doi.org/10.1016/0016-7037(94)90261-5.

[20] R.J. Myers, S.A. Bernal, J.L. Provis, A thermodynamic model for C-(N-)A-S-H gel: CNASH_ss. Derivation and validation, Cem. Concr. Res. 66 (2014) 27–47. https://doi.org/10.1016/J.CEMCONRES.2014.07.005.

[21] R.J. Myers, B. Lothenbach, S.A. Bernal, J.L. Provis, Thermodynamic modelling of alkali-activated slag cements, Appl. Geochemistry. 61 (2015) 233–247.

https://doi.org/10.1016/J.APGEOCHEM.2015.06.006.

[22] T. Matschei, B. Lothenbach, F.P. Glasser, Thermodynamic properties of Portland cement hydrates in the system CaO-Al_2O_3-SiO_2-$CaSO_4$-$CaCO_3$-H_2O, Cem. Concr. Res. 37 (2007) 1379–1410. https://doi.org/10.1016/j.cemconres.2007.06.002.

[23] H.C. Helgeson, J.M. Delany, H.W. Nesbitt, D.K. Bird, Summary and critique of the thermodynamic properties of rock-forming minerals, Am. J. Sci. 278A (1978) 229 pp.

[24] E.T. Turkdogan, J. Pearson, Thermodynamic functions of elements and compounds: Entropies of inorganic substances, J. Appl. Chem. 3 (1953) 495–501. https://doi.org/10.1002/jctb.5010031104.

[25] H.D.B. Jenkins, L. Glasser, Standard Absolute Entropy, S298o, Values from Volume or Density. 1. Inorganic Materials, Inorg. Chem. 42 (2003) 8702–8708. https://doi.org/10.1021/ic030219p.

[26] L. Glasser, H.D.B. Jenkins, Predictive thermodynamics for condensed phases, Chem. Soc. Rev. 34 (2005) 866–874. https://doi.org/10.1039/b501741f.

[27] L. Glasser, H.D.B. Jenkins, Predictive thermodynamics for ionic solids and liquids, Phys. Chem. Chem. Phys. 18 (2016) 21226–21240. https://doi.org/10.1039/c6cp00235h.

[28] L. Glasser, Thermodynamics of condensed phases: Formula unit volume, Vm, and the determination of the number of formula units, Z, in a crystallographic unit cell, J. Chem. Educ. 88 (2011) 581–585. https://doi.org/10.1021/ed900046k.

[29] H.D.B. Jenkins, L. Glasser, Thermodynamic difference rules: A prescription for their application and usage to approximate thermodynamic data, J. Chem. Eng. Data. 55 (2010) 4231–4238. https://doi.org/10.1021/je100383t.

[30] L. Glasser, H.D.B. Jenkins, Volume-based thermodynamics: A prescription for its application and usage in approximation and prediction of thermodynamic data, J. Chem. Eng. Data. 56 (2011) 874–880. https://doi.org/10.1021/je100683u.

[31] H.D.B. Jenkins, L. Glasser, Difference rule - A new thermodynamic principle: Prediction of standard thermodynamic data for inorganic solvates, J. Am. Chem. Soc. 126 (2004) 15809–15817. https://doi.org/10.1021/ja040137f.

[32] L.G. Baquerizo, T. Matschei, K.L. Scrivener, Impact of water activity on the stability of ettringite, Cem. Concr. Res. 79 (2016) 31–44. https://doi.org/10.1016/J.CEMCONRES.2015.07.008.

[33] Q. Zhou, F.P. Glasser, Thermal stability and decomposition mechanisms of ettringite at, Cem. Concr. Res. 31 (2001) 1333–1339. https://doi.org/10.1016/S0008-8846(01)00558-0.

[34] H. Taylor, Cement chemistry, 2nd ed., Thomas Telford Publishing,

London, 1997.

[35] T. Matschei, F.P. Glasser, Thermal stability of thaumasite, Mater. Struct. Constr. 48 (2015) 2277–2289. https://doi.org/10.1617/s11527-014-0309-4.

[36] T. Schmidt, B. Lothenbach, M. Romer, K. Scrivener, D. Rentsch, R. Figi, A thermodynamic and experimental study of the conditions of thaumasite formation, Cem. Concr. Res. 38 (2008) 337–349. https://doi.org/10.1016/j.cemconres.2007.11.003.

[37] B. Lothenbach, L. Pelletier-Chaignat, F. Winnefeld, Stability in the system CaO-Al_2O_3-H_2O, Cem. Concr. Res. 42 (2012) 1621–1634. https://doi.org/10.1016/j.cemconres.2012.09.002.

[38] L.G. Baquerizo, T. Matschei, K.L. Scrivener, M. Saeidpour, L. Wadsö, Hydration states of AFm cement phases, Cem. Concr. Res. 73 (2015) 143–157. https://doi.org/10.1016/j.cemconres.2015.02.011.

[39] I.G. Richardson, Clarification of possible ordered distributions of trivalent cations in layered double hydroxides and an explanation for the observed variation in the lower solid-solution limit, Acta Crystallogr. Sect. B Struct. Sci. Cryst. Eng. Mater. 69 (2013) 629–633. https://doi.org/10.1107/S2052519213027905.

[40] I.G. Richardson, The importance of proper crystal-chemical and geometrical reasoning demonstrated using layered single and double hydroxides, Acta Crystallogr. Sect. B Struct. Sci. Cryst. Eng. Mater. 69 (2013) 150–162. https://doi.org/10.1107/S205251921300376X.

[41] R.K. Allada, A. Navrotsky, J. Boerio-Goates, Thermochemistry of hydrotalcite-like phases in the MgO-Al_2O_3-CO_2-H2O system: A determination of enthalpy, entropy, and free energy, Am. Mineral. 90 (2005) 329–335. https://doi.org/10.2138/am.2005.1737.

[42] B. Lothenbach, L. Pelletier-Chaignat, F. Winnefeld, Stability in the system CaO–Al_2O_3–H_2O, Cem. Concr. Res. 42 (2012) 1621–1634.

[43] G. Möschner, B. Lothenbach, J. Rose, A. Ulrich, R. Figi, R. Kretzschmar, Solubility of Fe–ettringite (Ca6[Fe(OH)6]2(SO4)3 · 26H2O), Geochim. Cosmochim. Acta. 72 (2008) 1–18. https://doi.org/10.1016/J.GCA.2007.09.035.

[44] B.Z. Dilnesa, B. Lothenbach, G. Renaudin, A. Wichser, D. Kulik, Synthesis and characterization of hydrogarnet $Ca_3(Al_xFe_{1-x})_2(SiO_4)_y(OH)_{4(3-y)}$, Cem. Concr. Res. 59 (2014) 96–111. https://doi.org/10.1016/J.CEMCONRES.2014.02.001.

[45] B.Z. Dilnesa, B. Lothenbach, G. Le Saout, G. Renaudin, A. Mesbah, Y. Filinchuk, A. Wichser, E. Wieland, Iron in carbonate containing AFm phases, Cem. Concr. Res. 41 (2011) 311–323. https://doi.org/10.1016/J.CEMCONRES.2010.11.017.

[46] B.Z. Dilnesa, B. Lothenbach, G. Renaudin, A. Wichser, E. Wieland,

Stability of monosulfate in the presence of iron, J. Am. Ceram. Soc. 95 (2012) 3305–3316. https://doi.org/10.1111/j.1551-2916.2012.05335.x.

[47] B.Z. Dilnesa, Fe-containing hydrates and their fate during cement hydration: thermodynamic data and experimental study, EPFL, 2012.

[48] E. Gartner, T. Sui, Alternative cement clinkers, Cem. Concr. Res. 114 (2018) 27–39. https://doi.org/10.1016/j.cemconres.2017.02.002.

[49] R. Rinaldi, M. Sacerdoti, E. Passaglia, Stratlingite: crystal structure, chemistry, and a reexamination of its polytype vertumnite, Eur. J. Mineral. 2 (1990) 841–849. https://doi.org/10.1127/ejm/2/6/0841.

[50] E.W. D. Kulik, J. Tits, Aqueous-solid solution model of strontium uptake in C-S-H phases, Geochim. Cosmochim. Acta. 71 (2007) A530.

[51] D.A. Kulik, M. Kersten, Aqueous Solubility Diagrams for Cementitious Waste Stabilization Systems: II, End-Member Stoichiometries of Ideal Calcium Silicate Hydrate Solid Solutions, J. Am. Ceram. Soc. 84 (2001) 3017–3026. https://doi.org/10.1021/es010250v.

[52] D.A. Kulik, Improving the structural consistency of C-S-H solid solution thermodynamic models, Cem. Concr. Res. 41 (2011) 477–495. https://doi.org/10.1016/j.cemconres.2011.01.012.

[53] D. Nied, K. Enemark-Rasmussen, E. L'Hopital, J. Skibsted, B. Lothenbach, Properties of magnesium silicate hydrates (M-S-H), Cem. Concr. Res. 79 (2016) 323–332. https://doi.org/10.1016/j.cemconres.2015.10.003.

[54] B. Lothenbach, E. Bernard, U. Mäder, Zeolite formation in the presence of cement hydrates and albite, Phys. Chem. Earth. 99 (2017) 77–94. https://doi.org/10.1016/j.pce.2017.02.006.

[55] P. Blanc, P. Vieillard, H. Gailhanou, S. Gaboreau, N. Marty, F. Claret, B. Madé, E. Giffaut, ThermoChimie database developments in the framework of cement/clay interactions, Appl. Geochemistry. 55 (2015) 95–107. https://doi.org/10.1016/j.apgeochem.2014.12.006.

[56] T. Hanein, T.Y. Duvallet, R.B. Jewell, A.E. Oberlink, T.L. Robl, Y. Zhou, F.P. Glasser, M.N. Bannerman, Alite calcium sulfoaluminate cement: chemistry and thermodynamics , Adv. Cem. Res. 31 (2019) 94–105. https://doi.org/10.1680/jadcr.18.00118.

[57] T. Hanein, A. Elhoweris, I. Galan, F.P. Glasser, M.C. Bannerman, Thermodynamic data of ye'elemite (C_4A_3S) for cement clinker equilibrium calculations, in: Proc. 35th Cem. Concr. Sci. Conf., Aberdeen, UK, 2015.

[58] A. Cuesta, A.G. De La Torre, E.R. Losilla, V.K. Peterson, P. Rejmak, A. Ayuela, C. Frontera, M.A.G. Aranda, Structure, atomistic simulations, and phase transition of stoichiometric yeelimite, Chem.

Mater. 25 (2013) 1680–1687. https://doi.org/10.1021/cm400129z.

[59] E. Irran, E. Tillmanns, G. Hentschel, Ternesite, $Ca_5(SiO_4)_2SO_4$, a new mineral from the Ettringer Bellerberg/Eifel, Germany, Mineral. Petrol. 60 (1997) 121–132. https://doi.org/10.1007/BF01163138.

[60] D. Kurokawa, S. Takeda, M. Colas, T. Asaka, P. Thomas, K. Fukuda, Phase transformation of $Ca_4[Al_6O_{12}]SO_4$ and its disordered crystal structure at 1073 K, J. Solid State Chem. 215 (2014) 265–270. https://doi.org/10.1016/J.JSSC.2014.03.040.

[61] A. Kirfel, G. Will, Charge density in anhydrite, $CaSO_4$, from X-ray and neutron diffraction, Acta Crystallogr. B36 (1980) 2881–2890.

[62] W. Hörkner, H. Müller-Buschbaum, Crystal-structure of $CaAl_2O_4$, Inorg. Nucl. Chem. 38 (1976) 983–984.

[63] G. Álvarez-Pinazo, A. Cuesta, M. García-Maté, I. Santacruz, E.R. Losilla, A.G. De la Torre, L. León-Reina, M.A.G. Aranda, Rietveld quantitative phase analysis of Yeelimite-containing cements, Cem. Concr. Res. 42 (2012) 960–971. https://doi.org/10.1016/J.CEMCONRES.2012.03.018.

[64] ASTM E1269-11, Standard Test Method for Determining Specific Heat Capacity by Differential Scanning Calorimetry, West Conshohocken, PA, 2018.

[65] E. Gamsjäger, M. Wiessner, Low temperature heat capacities and thermodynamic functions described by Debye–Einstein integrals, Monatshefte Fur Chemie. 149 (2018) 357–368. https://doi.org/10.1007/s00706-017-2117-3.

[66] E. Gamsjäger, M. Morishita, H. Gamsjäger, Calculating entropies of alkaline earth metal molybdates, Monatshefte Fur Chemie. 147 (2016) 263–267. https://doi.org/10.1007/s00706-015-1588-3.

[67] W. Chase, NIST-JANAF Thermochemical Tables, 4th Ed., American Institute of Physics, New York, 1998.